Concentric Fe-oxyhydroxide bands in dacite cobbles : rates of buffering chemical reactions

Hidekazu Yoshida[1*], Nagayoshi Katsuta[2], Sin-ichi Sirono[3],
Shoji Nishimoto[4], Hirokazu Kawahara[5] & Richard Metcalfe[6]

1) Nagoya University, University Museum, Furocho, Aichi, Nagoya, Japan
*corresponding author) dora@num.nagoya-u.ac.jp
2) Faculty of Education, Gifu University, Gifu, Japan
3) Graduate School of Environmental Studies, Nagoya University, Nagoya, Japan
4) Nagoya City Science Museum, Nagoya, Japan
5) Japan Oil, Gas and Metals National Corporation (JOGMEC), Minato-ku, Tokyo, Japan
6) Quintessa, Videcom House, Newtown Road, Henley-on-Thames, Oxfordshire, UK

Abstract

'Liesegang patterns', rinds and bands are commonly observed in nature and form by self-organised periodic precipitation of Fe-oxyhydroxide following a nonlinear reaction-diffusion process. Although strictly Liesegang patterns consist of bands that increase in width with increasing distance from the source of the Fe that precipitated as Fe-oxyhydroxide, regular banded patterns are also sometimes observed that are otherwise similar to Liesegang patterns. However, the detailed process and time scale of regular Fe-oxyhydroxide bands development is still not fully understood. Here we describe an example of regular Fe-oxyhydroxide bands formed within dacite cobbles. Iron that was provided to the outer surfaces of the cobbles by acidic water that diffused towards the cobbles' cores. The spatial distributions of Ca and Fe within the Fe-oxyhydroxide bands across the cobbles show that the rhythmic Fe-oxyhydroxide precipitation was controlled by pH buffering. The width of each band (L) and the expected diffusion coefficient of the rock matrix (D) provide the rate of reaction (V) and allow us to estimate the duration of Fe-oxyhydroxide band formation. A 'diffusion-reaction cross plot' implies that the rhythmic Fe-oxyhydroxide patterns formed very rapidly, within an order of 10^2 - 10^3 years, considerably faster than previously estimated. The simplified model can be

applied to estimate the reaction time in any similar rock if regular Fe-oxyhydroxide bands are observed.

Key words; Liesegang patterns, Fe-oxyhydroxide, growth rate, pH buffering

1. Introduction

Liesegang rings are bands of a solid precipitate formed when one soluble substance diffuses into another which is dissolved in a gel. They were first described over a century ago by German chemist Raphael Liesegang (1896). Liesegang phenomena are now widely recognized in many natural and artificial situations in which a soluble substance diffuses into a reactive gel (Nabika et al., 2020).

Strictly, in a 'Liesegang Phenomenon' the spacing of the bands is not constant, but increases with distance from the source of diffusing solutes that precipitated to form the bands, according to a power law (e.g. Karam et al.,2011; Krug and Brandtstädter,1999). However, some Fe-oxyhydroxide rhythmic bands in rocks are regular, though in other respects are similar to 'Liesegang patterns'. These bands are considered to be 'fossilized' evidence of a water-rock interaction process by which soluble elements are precipitated in waves (e.g. Ortoleva, 1984; L'Heureux, 2013). Such rhythmic bands are often described as a 'zebra texture' (e.g. Dominic et al., 2017; Kelka et al., 2017) and are found in various rock types ranging from sedimentary rocks (e.g. Ortoleva, 1993; Fu et al., 1994; Wang et al., 2015) to igneous rocks (Yamamoto et al., 2013). The proposed formation mechanism involves weathering by dissolved iron-rich groundwaters that infiltrate the matrix of the rock through microscopic flow-paths. These flow-paths may consist of one or more types of pore space, including fracture porosity, inter-granular porosity, intra-granular porosity and secondary porosity (Yoshida et al., 2011). The iron-rich water participates in redox reactions and/or pH buffering reactions within the rock matrix, leading to the development of rhythmic features

such as a ‘Petra pattern’ that has been described in aeolian Jurassic sandstone (Abel et al., 2004) and ‘Zebra rock’ in Cambrian siltstone (Bevan, 2001). These patterns are known to form by complex diffusion-precipitation processes at reaction fronts (Msharrafieh et al., 2016, Sultan et al., 1990, Wang and Budd, 2012), but the detailed process is still little understood. Also, a methodology for confidently estimating the formation time of these rhythmic patterns is still lacking.

To address these issues, here we describe an example of Fe-oxyhydroxide banding formed in dacite cobbles from the Nagara River terrace, central Japan. The rhythmic Fe-oxyhydroxide bands form roughly concentric circles and were investigated to determine the processes and reaction time scales of their formation.

2. Studied materials and methods

All the sampled cobbles (25 samples) were collected from the Nagara River terrace in Gifu prefecture, central Japan. The cobbles have diameters of 15 to 25 cm and consist of dacite rocks with Fe-oxyhydroxide bands (Fig. 1a). The cobbles were transported by the Nagara River from the Cretaceous Okumino Acid Igneous Complex and Mesozoic Mino-terrain sedimentary rocks which are distributed in Gifu prefecture (Tanase, 1982; Wakita, 1984). The estimated age of the terrace deposit is ca. 7.3 ka based on the existence of a well-characterised marker, the Kikai-Akahoya (K-Ah) tephra (Yoshida and Wakita, 1999; Kitagawa et al., 1995). The concordance of the rhythmic Fe-oxyhydroxide bands with the outer surfaces of the dacite cobble indicates that the bands developed after the cobbles were formed and buried in the terrace deposit (Fig. 1).

To characterize the bands in the dacite cobbles, the microscopic occurrences of Fe-oxyhydroxide in the rock matrix were observed in thin-sections. Then, the mineralogy of the bulk felsic rock and the characteristics of the Fe-oxyhydroxide were determined by X-ray

diffractometer (XRD; Multiflex, Rigaku Co.) using crushed and powdered samples and Cu-Kα radiation (the Cu being subjected to an electron beam of 40 kV/20 mA).

All cobbles were cut to observe the internal bands, and a representative sample was selected for analysis. The analysis aimed to measure the elemental distribution on a plane surface through the centre of the cobble. The 2-D spatial distributions of Fe and other chemical constituents in this plane were carefully analysed semi-quantitatively by X-ray fluorescence analyzer (SXAM). The results were used to determine the width of the x-ray profile peak of each Fe-oxyhydroxide band quantitatively (Fig. 1).

The SXAM analyses were carried out using an X-ray fluorescence analyzer (XGT-2000V Horiba Japan) at the Department of Education, Gifu University, Gifu, Japan. A high-intensity continuous X-ray beam (Rh anode 50 kV 1 mA), 100μm in diameter, was focused with a guide tube and irradiated the surface of the sample perpendicularly. The sample was placed on a PC-controllable X-Y stage. X-ray fluorescence from the sample surface was analysed with the hp-Si detector of an energy-dispersion spectrometer (Katsuta et al., 2003).

3. Results

All dacite cobbles sampled from the Nagara River terrace have approximately concentric circular Fe-oxyhydroxide bands in the cores with similar band spacings (Figs.1a, b, d and f). Although the bands are sometimes intersected by fractures, as shown in Figure 1(a), basically circular bands are developed concordantly with the outer surface of the cobble.

Optical microscopic observations suggest that the cobbles were originally a holocrystalline intrusive felsic rock with small (< 5mm) phenocrysts of quartz and altered plagioclase in a matrix of mainly euhedral plagioclase (Figs. 1b and c). Petrographic microscopic observation shows that central parts of plagioclase phenocrysts, which are usually richer in Ca than the rims, are selectively replaced by sericite (Figs.1 c-1 and c-2).

XRD analysis shows no peaks of goethite nor lepidocrocite, suggesting that the Fe-oxyhydroxide observed microscopically is mostly amorphous. This phase has been precipitated in the inter-granular pores of the rock groundmass and grain boundary of rock forming minerals (Figs.1 b, c-1 and c-2). Although such precipitation of the Fe-oxyhydroxide reduced the sizes of micro-pores, the pore spaces form three-dimensional microscopic connected networks and were not entirely sealed by this process, but continued to act as diffusion pathways allowing the further development of the Fe-oxyhydroxide bands into the cores of the cobbles.

SXAM mapping shows one-dimensional element profiles produced along a section perpendicular to the concentric ring pattern characterised by Fe concentrations, as well as the distribution of Ca (Fig.1e). Profiles of other elements such as Mn, Si and K are also shown in the Supplementary. Elemental mapping revealed that Ca is depleted from the cobble and remains only in the core. In contrast Fe-oxyhydroxide bands formed from the outer part to the core have accumulated in the part of the cobble where Ca is depleted.

4. Discussion

4.1. Formation process of Fe-oxyhydroxide bands

The fact that the Fe-oxyhydroxide bands are concentric with the surfaces of the cobbles strongly suggests that the patterns formed after the cobbles were deposited in the river terrace. Had the Fe-oxyhydroxide rhythmic bands formed elsewhere then it is likely that they would have been cross-cut by the cobble surfaces owing to the effect of erosion during transport in the river. After the cobbles were deposited in the river terrace ca. 7.3 ka ago and buried to a depth of several metres, acidic water was supplied to the cobbles by the weathered organic rich soil that formed on the terrace (Yoshida and Wakita, 1999). The similarities of concentric

circular Fe-oxyhydroxide bands in cobbles suggest that in all cases the bands formed in cobbles under the same conditions after buried.

The Fe within the Fe-oxyhydroxide bands is considered as ferric. Since there is no oxidising agent within the cobbles, the Fe within the Fe-oxyhydroxide must have been transported to the cobbles in the Fe(III) form. This was possible owing to the acidic conditions developed within the soil of the terrace. The Fe was able to penetrate the cobbles by diffusion through the intact rock matrix and precipitate as Fe-oxyhydroxide periodically due to the buffering of pH towards more alkaline values by water / rock reactions within the cobbles. The solubility of Fe(III) varies from 2.2×10^{-5} mol/kg at pH = 4 to 2.5×10^{-8} mol/kg at pH=8, assuming equilibrium with $Fe(OH)_3$ (as calculated using PHREEQC and the thermodynamic databases “phreeqc.dat” (Parkhurst and Appelo, 2013)) for fresh water with redox buffered by the atmosphere.

The rhythmic Fe-oxyhydroxide bands are therefore considered as ‘fossilized’ evidence of the reaction-diffusion process. The widths of the bands (Fig.1 and Supplementary) also indicate the time intervals over which the process proceeded. The fact that among 10 - 20 period bands observed in each cobble, there is little variation in width or spacing, as identified from the Fe x-ray profile and SXAM (Figs.1d, e, f, g and Supplementary), suggests that the reaction rate was approximately constant. The Fe-oxyhydroxide was precipitated repeatedly during the diffusion of ferric iron from outside each cobble.

Within each Fe-oxyhydroxide band, the side closes to the core of the cobble has a darker reddish color than the side closest to the surface of the cobble. This variation indicates a greater accumulation of Fe towards the inner side of the band than the outer side of the band. This Fe concentration gradient in each band is also identified in the SXAM elemental maps and clearly shown by profile peak of measured Fe concentration (Figs.1d, f and g). The

textural features of the Fe-oxyhydroxide bands indicate that the Fe was provided continuously from the outsides of the cobbles and precipitated during diffusion into the rock groundmass.

The relationship between the Ca and Fe distributions can be explained by diffusion of acidic water from the cobble's surface into its core. This acidic water transported dissolved Fe, which was precipitated as pH increased due to reactions involving plagioclase. Other studies have shown that plagioclase dissolution can result in a low-pH condition (Oxburgh et al., 1994). The replacement of plagioclase suggests the dissolution and release of Ca to the pore water (Nishimoto and Yoshida, 2010). The dissolved Ca then diffused outwards through the pore-water leading to the cobble becoming depleted in Ca. These observations and geochemical analysis indicate that Fe was fixed to form Fe-oxyhydroxide bands as the Ferric iron-rich acidic water diffused inwards from the outer surfaces of the dacite cobbles. Precipitation of Fe-oxyhydroxide (here represented for simplicity by ferric hydroxide) will occur following;

$$Fe^{3+} + 3H_2O = 4Fe(OH)_3(s) + 3H^+ \quad \ldots\ldots\ldots\ldots (1)$$

The neutralization of acid by alteration of plagioclase will occur;

$$3CaAl_2Si_2O_8 + 2K^+ + 4H^+ = 3Ca^{2+} + 2KAl_3Si_3O_{10}(OH)_2 \ldots\ldots\ldots\ldots\ldots(2)$$

Combining the (1) and (2) reactions yields;

$$4Fe^{3+} + 12H_2O + 9CaAl_2Si_2O_8 + 6K^+ = 9Ca^{2+} + 6KAl_3Si_3O_{10}(OH)_2 + 4Fe(OH)_3 \ldots.(3)$$

Once the Fe-oxyhydroxide precipitated in the microscopic pores and connected porosity network, additional acidic water diffused further towards the core of the cobble along flow-paths that have not been clogged by Fe-oxyhydroxide and also through newly developed microscopic pores produced by plagioclase dissolution. Reaction (3) above will tend to produce a small amount of porosity (around 2.5 cm^3 per mol of plagioclase reacted, using data in the thermodynamic database thermo.dat, distributed with Geochemists Workbench; Bethke, 2008) because the reaction products have slightly lower molar volumes. Owing to these

effects, there will be little influence of fracture skins. The acidic water also contained Mn that precipitated in approximately the same locations as the Fe, producing a consistent correlation between Fe and Mn bands (Barnaby and Rimstidt, 1989; Supplementary).

On the basis of the above evidence, the following mechanism for Fe-oxyhydroxide band formation in the cobbles is summarized in Fig. 2: (1) the cobbles were buried in organic rich terrace sediments containing detrital Fe-rich shale clasts from the Mino-terrain (Wakita, 1988); (2) Fe in the terrace deposit was mobilized as ferric iron from the sediment by acidic water and was transported downwards to the cobbles, where it penetrated their groundmass (Fig. 2b (t1)); and (3) ferric iron transported in the acidic water was fixed to form Fe-oxyhydroxide bands due to pH buffering (Fig. 2b (t2)).

In step (2) the acidic water (pH < 3 ~ 4) was developed below the groundwater table by liberation of organic acids from the organic rich terrace sediments. Due to its low pH this water dissolved ferric iron from the weathered detrital Fe-rich shale clasts within the terrace deposit (Appelo and Postma, 1994). In step (3), as this water penetrated the dacite groundmass by diffusion, the water's pH increased due to buffering mainly by water-rock reactions involving plagioclase in the dacite rock groundmass. Reaction of the plagioclase consumed H^+, thereby increasing the pH at the front of penetrating acidic water and causing the mobilized ferric iron to precipitate in a band of Fe-oxyhydroxide at the front. As the supply of water containing Fe continues, the reaction front moves towards the core of the cobble and a new buffering reaction begins at a new front, where a new Fe-oxyhydroxide rich band forms (Fig. 2b (t3)). In this process, an Fe-oxyhydroxide band precipitates and new ferric iron inflows to the band. However, the acid water that flows to the band is already saturated with Fe in equilibrium with Fe-oxyhydroxide, just at a lower pH. Hence, it cannot dissolve any of the pre-precipiated Fe-oxyhydroxide. This step-wise progression of the reaction front continues to form rhythmic Fe-oxyhydroxide bands with certain rim widths

until the termination of the acidic water supply or the consumption of almost all feldspar within the groundmass.

4.2.Reaction time estimation

As the diffusion-controlled mechanism is responsible for the spherical Fe-oxyhydroxide bands studied here, it follows that the width of each band should reflect the rate of Fe-oxyhydroxide precipitation, with lower rates producing narrower bands. Therefore, the rhythmic Fe-oxyhydroxide pattern in the spherical intact rocks can be used to estimate the time of an individual band's formation as well as the overall formation time of the circular Fe-oxyhydroxide bands formed in a cobble.

Due to the clear concentration change of Fe-oxyhydroxide in the bands, the highest Fe concentration peaks are readily identified and the spacing between the bands can be measured (L: av. 3 ± 1 mm). Within the low-permeability igneous rock groundmass, any elemental mass transport is controlled by diffusion and therefore the width (L) can be used to estimate the duration of reaction (Figs.1g and f; Supplementary).

The acidic water penetrates the cobbles from outside. The speed of penetration of the reaction front is V. The penetration timescale required for the width of each band L is L/V. At the same time, ferric iron diffuses through the low pH water inward from the outside. The concentration of Fe in the rock at the penetration front gradually increases due to pH buffering and eventually exceeds the precipitation threshold, leading to the formation of a band of Fe-oxyhydroxide. The time required to exceed the threshold is given by the diffusion timescale of width L, given by L^2/D (D: diffusion coefficient of ferric iron in igneous rocks). Equating these two timescales leads to:

$$L = D/V \quad \ldots\ldots\ldots [1]$$

The penetration rate (V) at any time would be constant in a cobble, since there is a negligible temperature gradient across the cobble owing to its small size and also by the relatively homogenous intact rock groundmass. This means that a wider L is developed if the rock groundmass has a higher value of D and a narrower L is produced where the rock groundmass has a lower value of D. From the presently observed circular concentric Fe-oxyhydroxide banding pattern, we can determine L (3 mm average), corresponding to the development of rhythmic Fe-oxyhydroxide bands. The growth rate of the Fe-oxyhydroxide bands can be used to estimate the average width of each band. A growth timescale τ is given by:

$$\tau = R/V \quad \ldots\ldots\ldots [2]$$

where R is the radius of a cobble.

From equations [1] and [2], we can constrain the diffusion rate of relevant ions through the cobbles groundmass, and the timescale taken for an Fe-oxyhydroxide band to form, as shown in a 'Diffusion-reaction rate cross-plot' (Fig. 3). Published values of effective ferric iron diffusion coefficients in igneous rocks (e.g. 10^{-8} cm^2/s) with similar characteristics to those studied here (e.g. Arcos et al., 2006; Savage et al., 2009), can be used to estimate the minimum formation rate of an Fe-oxyhydroxide band. If the value of 3 mm is used, the expected formation time of an individual Fe-oxyhydroxide band would be within the order of 10^1 years. Therefore a 'Liesegang patterns' with multiple Fe-oxyhydroxide bands suggests that the overall reaction time within the cobbles is up to $10^2 \sim 10^3$ years at maximum. The timescales are much shorter than previously estimated (e.g.Yoshida et al., 2011).

Conclusion

In summary, the 'Diffusion-reaction rate cross-plot' with the values for 'L' obtained from 'Liesegang patterns' in dacite cobbles revealed that the record of short-term fluid-flow history

preserved in cementation patterns precipitated at fairly rapid time scales of rhythmic Fe-oxyhydroxide band growth. In particular, parametric analysis of transport processes shows that an individual band is only developed when diffusion occurs in combination with relatively rapid Fe-oxyhydroxide precipitation. The rhythmic Fe-oxyhydroxide pattern in a single cobble may have formed within a geologically very short time scale of $10^2 \sim 10^3$ years. The cross-plot also shows how conditions conducive to the formation of regular Fe-oxyhydroxide bands developed in the rock groundmass. The cross-plot can be applied to estimate the reaction time in similar types of rock in which regular Fe-oxyhydroxide bands, which are otherwise similar to 'Liesegang patterns' are observed.

CAPTIONS

Fig. 1 Occurrence of Fe-oxyhydroxide band. Cross-cut view of dacite cobble and Fe-oxyhydroxide bands (a). Fe-oxyhydroxide bands and Fe-oxyhydroxide precipitates in rock thin section. Fe-oxyhydroxide precipitated in rock groundmass (b) and feldspar grain (c-1: open, c-2: cross polar). Fe (d) and Ca (e) distribution in cobble measured by SXAM (cnt: X-ray intensity; count per second). Fe profile across the cobble (f) and measured intervals between each Fe peak (g).

Fig. 2 Formation process of Fe-oxyhydroxide bands in cobbles. Schematic image of Fe-oxyhydroxide band formation in dacite cobble after burial in organic rich terrace sediments (a). A model for Fe-oxyhydroxide band formation (b). t1: Beginning of the formation at the cobble surface. t2; Fe-oxyhydroxide band grown at a certain distance from the cobble surface because of sufficient pH buffering. t3; After Fe-oxyhydroxide precipitation, the reaction front moves to a deeper point and forms the next Fe-oxyhydroxide band by a reaction between the rock and acidic water. Fe-oxyhydroxide

279 bands are successively developed until the termination of the source fluid supply
280 and/or the consumption of feldspar.
281
282 **Fig. 3 Diffusion–growth rate cross-plot.** The relationship between L (width of reaction
283 front), D (diffusion coefficient of ferric iron in igneous rocks), and V (linear growth
284 rate of reaction front) can be written as L = D/V. The relationship between the
285 effective diffusion coefficient (D; cm^2/s) and the growth rate of Fe-oxyhydroxide
286 bands (V; cm/s) is defined by dimension analysis. The width (L:0.3cm) and the
287 effective diffusion coefficient of ferric iron in similar kinds of igneous rocks show a
288 very rapid growth rate of multiple Fe-oxyhydroxide bands within an order of 10^2 - 10^3
289 years.
290
291 **Declaration of competing interest**
292 The authors declare that they have no known competing financial interests or personal
293 relationships that could have appeared to influence the work reported in this paper.
294
295 **Acknowledgements**
296 We thank for helpful discussions and comments of the manuscript to Prof. K. Yamamoto of
297 Nagoya University and Prof. M. Chan of Utah University. We are also grateful to Mr. S. Yogo
298 of Nagoya University for preparing rock thin-sections, SXAM analyses. Three anonymous
299 reviewers' constructive comments are gratefully acknowledged. The research was supported
300 by JSPS KAKENHI grant 15H052227.
301
302 **Appendix A. Supplementary data**
303 Supplementary data associated with this article can be found, in the online version.

304

305 **References**

306 Abel, A.M., Atallah, M., Al-Masri, A., 2004. Active tectonism along the Dead Sea transform
307 in Jordan. Field Guide Book of 32nd International Geological Congress P03.
308 Appelo, C.A.J., Postma, D., 1994. Geochemistry, Groundwater and Pollution. A.A.Bakema
309 Rotterdam. 536p.
310 Acros, D., Grandia, F., Domenech, C., 2006. Geochemical evolution of the near field of a
311 KBS-3 repository. SKB Technical Report TR-06-16.
312 Barnaby, R.J., Rimstidt, J.D.,1989. Redox conditions of calcite cementation interpreted from
313 Mn and Fe contents of authigenic calcites. Geological Society of America Bulletin. 101,
314 795-804.
315 Bethke, C.M., 2008. Biogeochemical reaction modelling (2nd edition). Cambridge University
316 Press. Cambridge.
317 Bevan, A.W.R., 2001. Zebra rock: An ornamental stone from the east Kimberley, western
318 Australia. Australian Gemmologist. 21, 165-168.
319 Dominic, P., Zhenbing, S., Matthew, S.D., 2017. Chemically-oscillating reactions the
320 diagenetic oxidation of organic matter and in the formation of granules in late
321 Palaeoproterozoic chert from Lake Superior. Chemical geology. 470, 33-54.
322 Fu, L., Milliken, J., Sharp, J.M., 1994. Porosity and permeability variations in fractured and
323 liesegang-banded Breathitt sandstones (Middle Pennsylvanian), eastern Kentucky;
324 diagenetic controls and implications for modelling dual-porosity systems. Journal of
325 Hydrology. 154, 351-381.
326 Karam, T., El-Rassy, R., Sultan, R., 2011. Mechanism of Revert Spacing in a
327 $PbCrO_4$ Liesegang System. Jour. Phys. Chem. A, 115, 2994 – 2998.

328 Katsuta, N., Takano, M., Okaniwa, T. Kumazawa, M., 2003. Image processing to extract
329 sequential profiles with high spatial resolution from the 2D map of deformed laminated
330 patterns. Computers & Geosciences. 29, 725-740.
331 Krug, H-J., Brandtstädter, H., 1999. Morphological Characteristics of Liesegang Rings and
332 Their Simulations. Jour. Phys. Chem. A, 103, 7811- 7820.
333 Kelka, U., Veveakis, M., Koehn, D., Beaudoin, N., 2017. Zebra rocks: compaction waves
334 create ore deposits. Scientific Reports. 7, 14260; doi: 10.1038/serp41598-017-14541-3.
335 Kitagawa, H., Fukusawa, H., Nakamur, T., Okamura, M., Takemura, K., Hayashida, A.,
336 Yasuda, Y., 1995. AMS 14C dating of varved sediments from Lake Suigetsu, central
337 Japan and atmospheric 14C change during the late Pleistocene. Radiocarbon. 37, 371-378.
338 Liesegang, R. E., 1896. Über Einige Eigenschaften von Gallerten. Naturwiss. Wochenschr. 11,
339 353-362.
340 L'Heureux, I., 2013. Self-organized rhythmic patterns in geochemical systems. Philosophical
341 Transactions of The Royal Society, London, A. 371:20120356.
342 Msharrafieh, M., Al-Ghoul, M., Zaknoun, F., El-Rassy, H., El-Joubeily, S., Sultan, R., 2016.
343 Simulation of geochemical banding I: Acidization-precipitation experiments in a
344 ferruginous limestone rock. Chemical Geology. 440, 42-49.
345 Nabika, H., Itatani, M., Lagzi, I., 2020. Pattern formation in precipitation reactions: The
346 Leisegang Phenomenon. Langmuir. 36, 481-497.
347 Nishimoto, S., Yoshida, H., 2010. Hydrothermal alteration of deep fractured granite: Effects
348 of dissolution and precipitation. Lithos. 115, 153-162.
349 Orloleva, P.J., 1984. The self-organization of liesegang bands and other precipitate patterns. In
350 Chemical instabilities: applications in chemistry, engineering, geology, and materials
351 science. (ed. G.Nicols & F.Baras). 289-297.

352 Orloleva, P.J., 1993. Self-organization and nonlinear dynamics in sedimentary basins.
353 Philosophical Transactions of The Royal Society, London, A. 344, 171-179.
354 Oxburgh, R., Drever, J.I., Sun, Y-T., 1994. Mechanism of plagioclase dissolution in acid
355 solution at 25℃Geochemica Cosmochemica Acta. 58, 661-669.
356 Parkhurst, D.L., Appelo, C.A.J., 2013. Description of input and examples for PHREEQC
357 version 3-A computer program for speciation, batch-reaction, one-dimensional transport,
358 and inverse geochemical calculations: U.S. Geological Survey Techniques and Methods,
359 book 6, Chap. A43, 497 p., available only at http://pubs.usgs.gov/tm/06/a43.
360 Robinson, N.I., Sharp, J.M., Jr., Kreisel, I., 1998. Contaminant transport in sets of parallel
361 finite fractures with fracture skins. Jour. Contaminant Hydrology, 31, 83-109.
362 Savage, D., Watson, C., Wilson, J., Bond, A.E., Jones, W., Metcalfe, R., Milodowski, A.E.,
363 Munro, S., Penfold, J., Watson, S.P., 2009. Understanding radionuclide migration from
364 the D1225 shaft, Dounreay, Caithness, UK. Material Research Society Symposium
365 Proceedings. 1193, 367-374.
366 Sultan, R., Ortoleva, F., DePasquale, F., Tartaglia,P., 1990. Bifurcation of the Oswald-
367 Liesegang supersaturation-nucleation-depletion cycle. Earth Science reviews. 29, 163-
368 173.
369 Tanase, A., 1982. Okumino Acid Igneous Complex: Cretaceous Igneous Activity in the
370 Ryohaku Mountains, Central Japan. Journal of the Geological Society of Japan. 88, 271-
371 288 (in Japanese with English abstract).
372 Wakita, K., 1984. Geology of the Hachiman district. Quadrangle Series, scale 1 : 50,000.
373 Geological Survey of Japan, 89p. (in Japanese with English abstract, 6p.).
374 Wakita, K., 1988. Origin of chaotically mixed rock bodies in the Early Jurassic to Early
375 Cretaceous sedimentary complex of the Mino terrain, central Japan. Bulletin of
376 Geological Survey of Japan. 39, 675-757.

377 Wang, Y., Budd, D.A., 2012. Stress-induced chemical waves in sediment burial diagenesis.
378 Nature Communication. 3:685 doi:10.1038/ncomms1684.
379 Wang, Y., Chan, M., Merino, E., 2015. Self-organized iron-oxide cementation geometry as an
380 indicator of paleo-flows. Scientific Reports, 5, 10792; doi: 10.1038/serp10792.
381 Yamamoto, K., Yoshida, H., Akagawa, F., Nishimoto, S., Metcalfe, R., 2013. Redox front
382 penetration in the fractured Toki Granite, central Japan: An analogue for redox reactions
383 and redox buffering in fractured crystalline host rocks for repositories of long-lived
384 radioactive waste. Applied geochemistry. 35, 75-87.
385 Yoshida, F., Wakita, K., 1999. Geology of Gifu district. With Geological sheet map at
386 1:50,000. Geological Survey of Japan, 71p. (in Japanese with English abstract, 4p.).
387 Yoshida, H., Metcalfe, R., Nishimoto, S., Yamamoto, H., Katsuta, N., 2011. Weathering rind
388 formation in buried terrace cobbles during periods of up to 300ka. Applied Geochemistry,
389 26, 1706-1721.
390

Figure 1

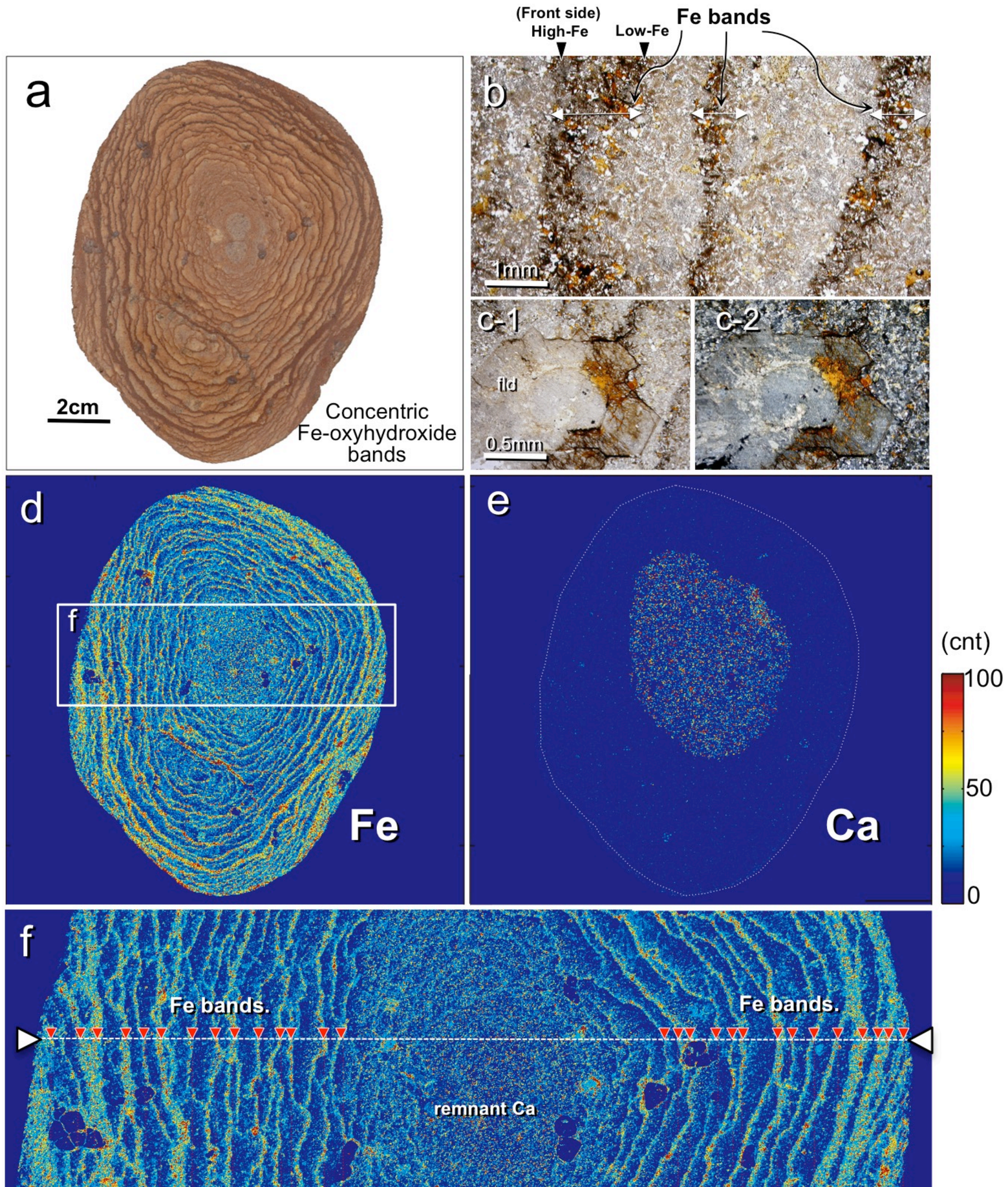
a
2cm
Concentric
Fe-oxyhydroxide
bands
(Front side)
High-Fe
Low-Fe
Fe bands
b
1mm
c-1
fld
0.5mm
c-2
d
f
Fe
e
Ca
(cnt)
100
50
0
f
Fe bands.
Fe bands.
remnant Ca
1cm
(cnt)
g
75
50
25
0
0
20
40
60
80
100
120
140
(mm)
Fe-oxyhydroxide bands
Fe-oxyhydroxide bands

Figure 2

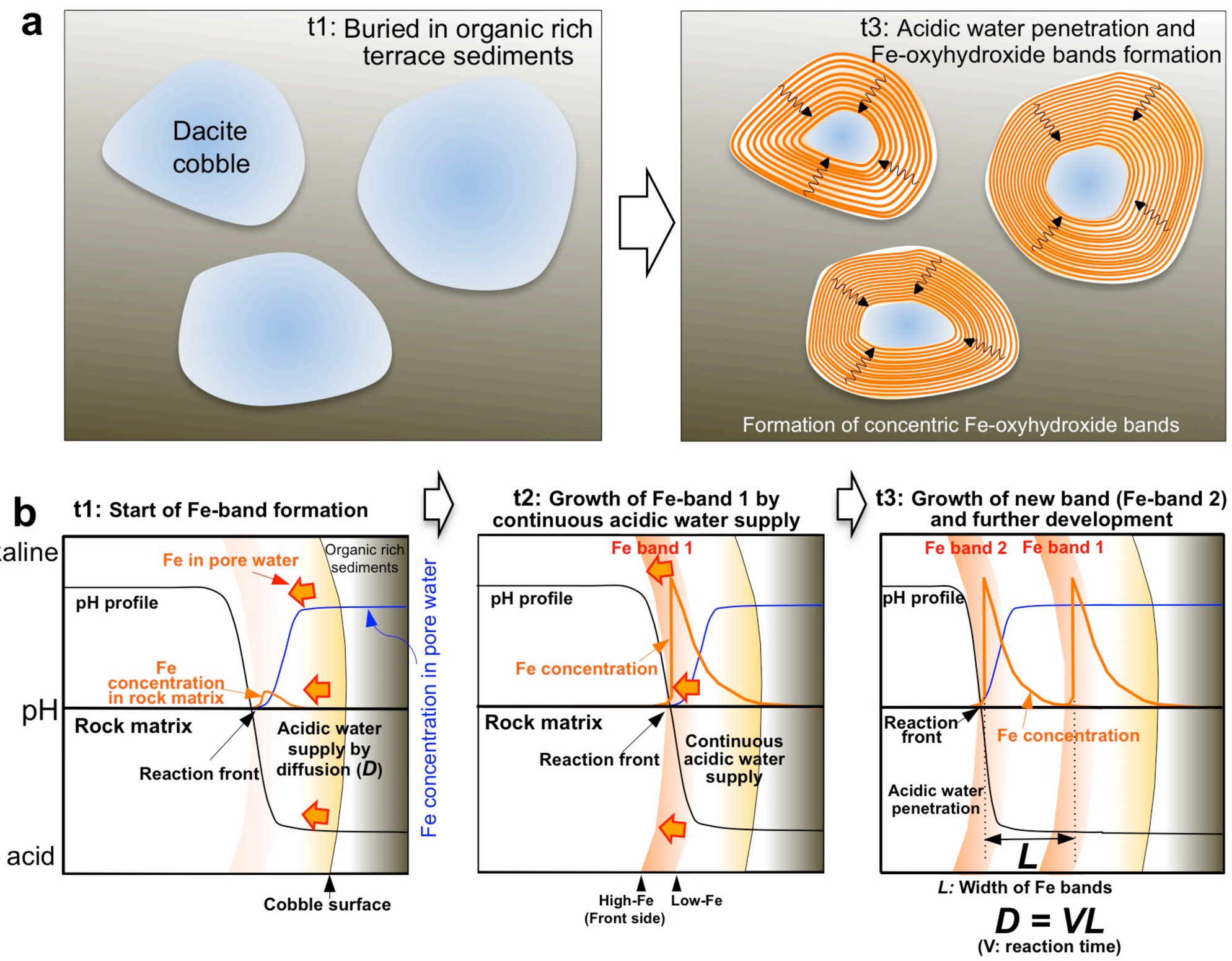
a
t1: Buried in organic rich terrace sediments
Dacite cobble
t3: Acidic water penetration and Fe-oxyhydroxide bands formation
Formation of concentric Fe-oxyhydroxide bands
b
t1: Start of Fe-band formation
alkaline
pH
acid
Fe in pore water
Organic rich sediments
pH profile
Fe concentration in rock matrix
Rock matrix
Reaction front
Acidic water supply by diffusion (D)
Cobble surface
Fe concentration in pore water
t2: Growth of Fe-band 1 by continuous acidic water supply
Fe band 1
pH profile
Fe concentration
Rock matrix
Reaction front
Continuous acidic water supply
High-Fe (Front side)
Low-Fe
t3: Growth of new band (Fe-band 2) and further development
Fe band 2
Fe band 1
pH profile
Reaction front
Fe concentration
Acidic water penetration
L
L: Width of Fe bands
D = VL
(V: reaction time)

Figure 3

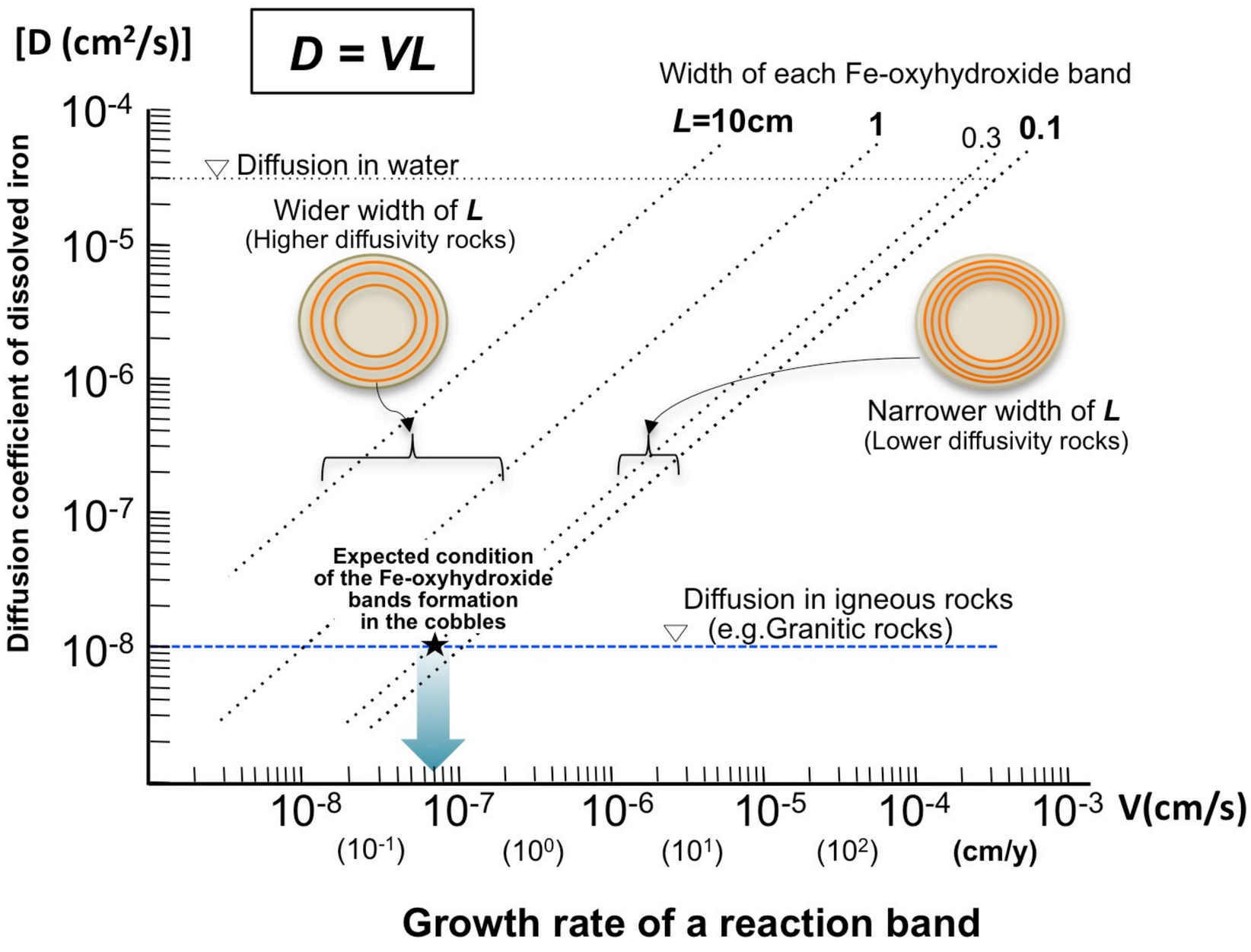
[D (cm²/s)]
D = VL
Width of each Fe-oxyhydroxide band
L=10cm
1
0.3
0.1
Diffusion coefficient of dissolved iron
10-4
10-5
10-6
10-7
10-8
Diffusion in water
Wider width of L
(Higher diffusivity rocks)
Narrower width of L
(Lower diffusivity rocks)
Expected condition
of the Fe-oxyhydroxide
bands formation
in the cobbles
Diffusion in igneous rocks
(e.g.Granitic rocks)
10-8
10-7
10-6
10-5
10-4
10-3
V(cm/s)
(10-1)
(100)
(101)
(102)
(cm/y)
Growth rate of a reaction band